

Soft Matter

Accepted Manuscript



This is an *Accepted Manuscript*, which has been through the Royal Society of Chemistry peer review process and has been accepted for publication.

Accepted Manuscripts are published online shortly after acceptance, before technical editing, formatting and proof reading. Using this free service, authors can make their results available to the community, in citable form, before we publish the edited article. We will replace this *Accepted Manuscript* with the edited and formatted *Advance Article* as soon as it is available.

You can find more information about *Accepted Manuscripts* in the [Information for Authors](#).

Please note that technical editing may introduce minor changes to the text and/or graphics, which may alter content. The journal's standard [Terms & Conditions](#) and the [Ethical guidelines](#) still apply. In no event shall the Royal Society of Chemistry be held responsible for any errors or omissions in this *Accepted Manuscript* or any consequences arising from the use of any information it contains.

Cite this: DOI: 10.1039/xxxxxxxxxx

Confined semiflexible polymers suppress fluctuations of soft membrane tubes

Sina Mirzaeifard^a and Steven M. Abel^{1*^a}Received Date
Accepted Date

DOI: 10.1039/xxxxxxxxxx

www.rsc.org/journalname

We use Monte Carlo computer simulations to investigate tubular membrane structures with and without semiflexible polymers confined inside. At small values of membrane bending rigidity, empty fluid and non-fluid membrane tubes exhibit markedly different behavior, with fluid membranes adopting irregular, highly fluctuating shapes and non-fluid membranes maintaining extended tube-like structures. Fluid membranes, unlike non-fluid membranes, exhibit a local maximum in specific heat as their bending rigidity increases. The peak is coincident with a transition to extended tube-like structures. We further find that confining a semiflexible polymer within a fluid membrane tube reduces the specific heat of the membrane, which is a consequence of suppressed membrane shape fluctuations. Polymers with a sufficiently large persistence length can significantly deform the membrane tube, with long polymers leading to localized bulges in the membrane that accommodate regions in which the polymer forms loops. Analytical calculations of the energies of idealized polymer-membrane configurations provide additional insight into the formation of polymer-induced membrane deformations.

1 Introduction

Cell biology is replete with examples of polymers confined by flexible membranes. For example, the persistence length of biopolymers such as actin ($l_p \approx 15 \mu\text{m}$) and double-stranded DNA ($l_p \approx 50 \text{ nm}$) can be much larger than the characteristic size of the membrane-surrounded region in which they are confined.^{1–7} When polymers are confined by membranes, there is often a non-trivial interplay between elastic properties of the membrane, the size and shape of the confining region, and the length and stiffness of the confined polymer. In this work, we are conceptually motivated by membrane nanotubes, which are tubular membrane structures that contain actin and connect cells over long distances (~ 10 to $100 \mu\text{m}$).^{8–12} Disrupting the actin cytoskeleton abrogates membrane nanotubes by an unknown mechanism, making them an interesting model system for studying membrane-polymer interactions. It is speculated that cells use membrane nanotubes to communicate over long distances, and viruses have been shown to exploit membrane nanotubes to propagate from one cell to another. Other tubular membrane structures, such as those occurring in organelles and cell protrusions, are also common in cells, and membrane tubes can be formed readily in many experimental studies as well.^{13–15}

In this study, we use a continuum framework to study semiflexible polymers confined within elastic membrane tubes. A semi-

flexible polymer is represented by the curve $r(s)$, and its energy is given by

$$\mathcal{H}_p = \frac{l_p k_B T}{2} \int_0^l ds \left(\frac{\partial^2 r(s)}{\partial s^2} \right)^2, \quad (1)$$

where l_p is the persistence length of the polymer, $k_B T$ is the thermal energy, and l is the total length of the polymer. The energy of the membrane is given by the Helfrich free energy,

$$\mathcal{H}_m = \frac{\kappa}{2} \int dA (H - H_0)^2, \quad (2)$$

where κ is the bending rigidity, $H = C_1 + C_2$, C_1 and C_2 denote the two principal curvatures at a point on the membrane, and H_0 is the intrinsic curvature, which we take to be zero in this study. The integral is computed over the entire membrane surface, and we neglect a term associated with Gaussian curvature since we are interested in membranes of fixed topology. The bending energy of the polymer and membrane can also be captured using discrete representations of the polymer and membrane, as described below (the discrete representations are amenable to computer simulation methods).

Elastic membranes have been studied extensively using both theory and computer simulations (for a thorough review on the statistical mechanics of membranes, see Ref.¹⁶). Membranes are typically characterized by their fluidity: Non-fluid membranes (often called polymerized or tethered membranes) maintain internal connectivity and resist in-plane shear, while fluid mem-

^a Department of Chemical and Biomolecular Engineering, University of Tennessee, Knoxville, Tennessee 37996, USA. E-mail: abel@utk.edu

branes exhibit fluidity of constituent components and do not resist in-plane shear. Early theoretical work focused on characterizing the shape and roughness of membranes, especially at low bending rigidity, where thermal fluctuations can dramatically influence membrane shape. Studies have focused on the crumpling transition in polymerized membranes,¹⁷ roughness in self-avoiding polymerized membranes,^{18,19} and characterization of the shape of fluid membranes.^{20–24} Fluid vesicles have been found to exhibit a branched-polymer-like phase at small values of the bending rigidity. In this regime, entropic gains obtained by forming fingerlike projections outweigh their modest energetic costs.^{25,26}

Semiflexible polymers have received considerable attention in part because of their relevance in studying properties of biomolecules such as DNA.^{5,7,27,28} A number of theoretical and computational studies have investigated semiflexible polymers under both hard^{2–5,29,30} and soft tubular confinement.^{1,6,31} Studies of semiflexible polymers under soft tubular confinement have characterized the shape and diffusion of a model polymer within a polymerized membrane tube,³¹ shown that a semiflexible polymer can prevent a filopodial projection from collapsing,¹ and developed scaling relationships for constructing qualitative phase diagrams of polymers confined within fluid tubes.⁶ In a related study, Fošnarič et al. considered a single semiflexible polymer confined within a fluid vesicle and showed that sufficiently stiff polymers deform the membrane into a disk-like shape, which is in contrast with the spherical shape of an empty fluid membrane at moderate bending rigidity.³²

In this paper, we use computer simulations to explore the equilibrium behavior of elastic membrane tubes and confined semiflexible polymers. In contrast with previous work, we explore the effects of membrane fluidity and bending rigidity on the behavior of membrane tubes. We also investigate the interplay of a confined polymer and the membrane for a variety of polymer sizes and persistence lengths. The paper is organized as follows: After introducing the discrete models of polymers and membranes, we compare the behavior of polymerized and fluid tubular membrane structures. The fluid tubes exhibit qualitatively different behavior at small values of the bending rigidity, where they are characterized by large fluctuations in membrane shape. We then explore how confining a semiflexible polymer within the tube influences the behavior of the membrane, finding that the presence of the polymer suppresses fluctuations of the membrane and can lead to localized deformations of the tube where the polymer forms loops.

2 Methods

We use Monte Carlo computer simulations to explore the equilibrium behavior of elastic membrane tubes with and without confined semiflexible polymers. In the simulations, we use discretized representations of the polymer and membrane that have been used widely in a variety of studies and that are amenable to computer simulation (see, for example, refs.^{31–33}).

The polymer consists of M particles connected by $M - 1$ bonds. The bond length can range from $l_{\min} = \sigma$ to $l_{\max} = 1.67\sigma$, and the

energy of the polymer is given by³²

$$E_p = \lambda_p \sum_{j=1}^{M-2} (1 - \cos \theta_j),$$

where θ_j denotes the angle between two successive bonds and $\lambda_p = l_p k_B T / \bar{l}$, with l_p the effective persistence length and $\bar{l} = (l_{\min} + l_{\max})/2$. For this study, we neglect excluded volume interactions between polymer particles. In a similar manner, the membrane is represented as a triangulated surface that consists of N particles connected by bonds. As with the polymer, bond lengths can range from l_{\min} to l_{\max} . All membrane particles, including those not connected by bonds, interact by a hard-sphere potential with each particle having a hard-sphere diameter of l_{\min} . The bending energy is given by

$$E_m = \lambda_m \sum_{(i,j)} (1 - \mathbf{n}_i \cdot \mathbf{n}_j),$$

where the sum extends over all pairs of triangles sharing a bond, \mathbf{n}_i denotes a normal vector to triangle i , and λ_m is related to the bending rigidity by $\lambda_m = 2\kappa/\sqrt{3}$. This form of the energy has been used widely for triangulated surfaces,^{16,17,22,25} and the definition of λ_m holds for cylindrical surfaces.^{16,22} The polymer and membrane interact through hard-sphere interactions of their constituent particles, which each having a hard-sphere diameter of l_{\min} . We consider both fluid membranes and non-fluid membranes. Non-fluid membranes maintain a fixed connectivity of particles.^{16,17} In contrast, the connectivity of fluid membranes is not fixed, allowing particles to change their neighbors and move throughout the membrane.^{16,19,25}

We employ Metropolis Monte Carlo computer simulations to sample equilibrium configurations of polymer-membrane systems described by the energy functions above. Denoting the total energy by $E = E_p + E_m$, trial configurations are accepted with probability 1 if $\Delta E = E_{\text{trial}} - E_{\text{current}} \leq 0$ and with probability $\exp(-\Delta E/k_B T)$ otherwise. Monte Carlo updates include two types of trial moves: In the first, a particle is selected from either the polymer or membrane and its position is randomly updated, with a maximum displacement of $0.15 l_{\min}$. This choice of maximum displacement ensures that the polymer will not pass through the membrane surface during the simulation. In the second type of trial update, the connectivity of the membrane is updated using a bond-flip move in which a randomly chosen bond is cut and replaced by a new bond.^{16,19,25} The new bond connects the two initially unconnected particles associated with the triangles sharing the original bond. New bonds must satisfy the bond length constraint and each particle involved must have at least three bonds to other particles. The bond-flip update incorporates fluidity into the membrane. A single Monte Carlo sweep for a non-fluid membrane consists of $M + N$ attempted moves of polymer particles and $M + N$ attempted moves of membrane particles. Attempts alternate between the polymer and the membrane, with a particle selected at random for each update attempt. For fluid membranes, a Monte Carlo sweep consists of an additional N bond-flip attempts, with a bond selected at random for each attempt.

To mimic a tubular extension connecting two cells, we consider

two parallel planes (representing the cell surfaces) separated by a fixed distance. Each end of the tubular membrane is constrained to move only within one of the planes. The initial configuration of the membrane is chosen to be cylindrical, with n_1 layers each containing n_p particles equally spaced along the circumference of the cylinder. The n_1 layers are equally spaced and span the distance between the two constraining planes, and the particles are arranged so as to form equilateral triangles with sides of length \bar{l} . The total number of triangles is $2n_p(n_1 - 1)$ and the distance between the planes is $(\sqrt{3}/2)(n_1 - 1)\bar{l}$, which accommodates the initial length of the membrane tube. The polymer is confined within the tube, and unless otherwise noted, each end of the polymer is constrained to move only within the same plane as the tube ends, leading to a polymer that extends the entire length of the tube. The initial configuration of the polymer is chosen to be a helix that spans the entire tube. To make connections with length scales relevant to cell biology, we let $\sigma = 1 \mu\text{m}$ and report polymer persistence lengths in units of μm . The smallest nonzero persistence length considered in this study is greater than three times the initial radius of the membrane tube.

For all simulation results, we average the quantities of interest over 10^6 Monte Carlo sweeps after allowing the system to equilibrate. Energies are calculated using the expressions above, and the specific heat of the membrane is given by

$$C = \frac{1}{N} \frac{1}{k_B T^2} \left(\langle E_m^2 \rangle - \langle E_m \rangle^2 \right)$$

The specific heat has been used to study fluctuations and roughness of triangulated membranes in previous studies.^{16,17,20,25}

3 Results

3.1 Energetics of empty membrane tubes

We begin by considering the behavior of empty membrane tubes, with an initial focus on the effects of membrane fluidity and of constraining the ends of the tube. Figure 1 characterizes the average energy of a membrane tube as a function of bending rigidity (κ). Note that the average energy of the membrane is not equivalent to the free energy of the system, which is minimized at thermal equilibrium, and that entropic contributions may significantly influence equilibrium configurations sampled by a membrane tube. The membrane contains $N = 1596$ particles initially arranged into 84 layers of 19 particles. In Fig. 1a, the energy of a non-fluid membrane tube is shown for two cases: (i) the ends of the tube are constrained to move in-plane only and (ii) the ends are free to move with no constraints. The mean energy is strictly increasing as a function of κ , with similar values for the constrained and unconstrained membrane tubes. The similarity in the average energy can be understood by noting that the fixed connectivity of particles in non-fluid membranes limits the tube from adopting shapes that deviate significantly from cylindrical. At sufficiently large values of the bending rigidity, local fluctuations in shape become less prominent, and the membrane tube can be regarded as approximately cylindrical. Using the Helfrich free energy (\mathcal{H}_m) defined previously and performing the integral over the surface of a cylinder, the total bending energy of a cylin-

der is $\pi\kappa L/R$, where R is the radius of the cylinder and L is the total length. Thus, with R and L fixed, the energy increases linearly with κ .

The behavior of a fluid membrane is qualitatively different, as depicted in Fig. 1b. For both the constrained and unconstrained cases, there is a local maximum in the average energy at small values of κ . This feature is not present in the non-fluid membrane tube. Additionally, for larger values of κ , the average energies of the constrained and unconstrained membrane tubes deviate significantly from one another, with the energy of the unconstrained membrane remaining relatively low. In this regime, as can be seen from the snapshots of configurations with $\kappa = 40 k_B T$, the constrained tube maintains a tubular shape while the unconstrained membrane adopts an approximately spherical shape. As with the cylindrical case, the Helfrich free energy can be readily computed for a sphere, giving a total energy of $8\pi\kappa$ (at fixed κ , spheres have the same total bending energy, independent of their radius). The spherical shape is energetically favorable at large values of κ , when thermal fluctuations are less prominent and entropic contributions play a less significant role. Note that the constrained fluid membrane tube at $\kappa = 40 k_B T$ has lower average energy than the non-fluid membrane tubes. This is due to the ability of the fluid membrane to change its connectivity and rearrange particle locations to adopt shapes that are less energetically costly, even while maintaining a tubular morphology.

3.2 Fluid membrane tubes exhibit a peak in specific heat at small κ

Figure 1b exhibits a local maximum in the average energy as a function of κ . We observe similar behavior for two additional tube sizes ($n_1 \times n_p$): $N = 1197$ (63×19) and $N = 798$ (42×19). To further characterize the behavior of empty membrane tubes, we calculate the specific heat of the membrane, which is shown as a function of κ in Figure 2 for the case with $N = 1197$. Comparing non-fluid and fluid membranes reveals that the specific heat of non-fluid membranes strictly increases as a function of κ (for small κ) while the fluid membrane exhibits a peak near $\kappa = 1.25 k_B T$. The peak observed for the fluid membrane is similar to behavior reported for fluid membrane vesicles.^{16,20,25,26} For the fluid vesicles, the peak was identified as indicating a transition from branched-polymer-like behavior at small κ to an extended, roughly spherical shape at large κ . Similar behavior is observed in the fluid membrane tubes studied here.

Figure 3 displays images taken from simulation trajectories of empty membrane tubes at various values of bending rigidity. Large-scale shape fluctuations are present for the fluid case with $\kappa = 0.25 k_B T$ and become less pronounced as κ is increased. We observe qualitatively similar behavior to that reported for fluid vesicles: At small values of κ , the membrane tube adopts conformations that exhibit fingerlike extensions. As κ increases, the membrane transitions to an extended tube-like state. This transition is consistent with the location of the local maximum in the specific heat. It is interesting that the fluid membrane tube exhibits the same qualitative behavior as fluid vesicles, as the tubes are constrained on both ends and have less freedom to make large

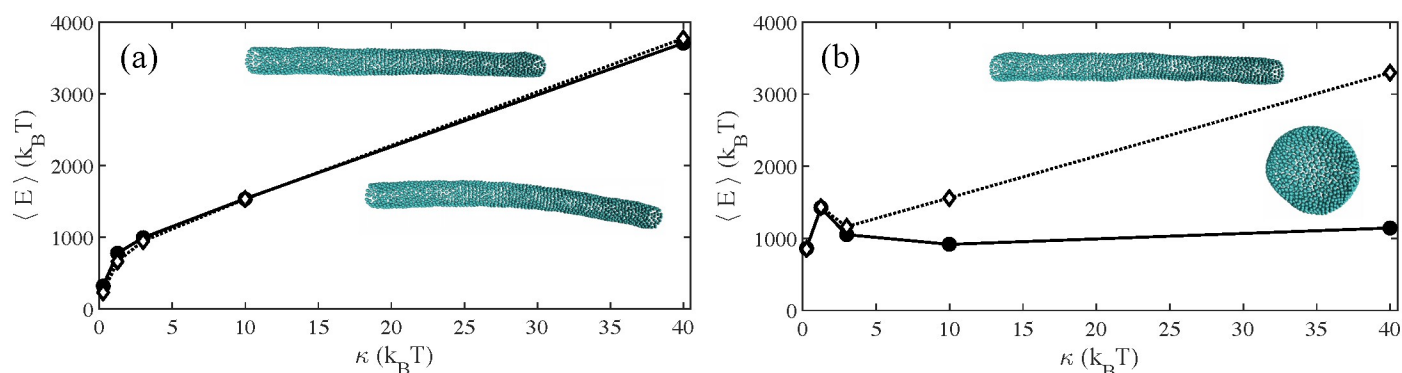


Fig. 1 Average energy of a membrane tube as a function of bending rigidity. The membrane contains $N = 1596$ particles, initially arranged to triangulate a cylinder with 84 layers of 19 particles per layer. Simulation results are shown for (a) non-fluid membranes and (b) fluid membranes. In each figure, results are shown for membrane tubes with both ends constrained (open diamonds) and both ends unconstrained (circles). A representative equilibrium configuration is shown for each case for $\kappa = 40 k_B T$ (constrained tubes are at the top). The unconstrained fluid membrane adopts a nearly spherical shape at large κ , leading to an average energy that is significantly smaller than in the other cases.

deformations while maintaining the full tube length. Non-fluid membranes do not show the same large-scale shape fluctuations, which is a result of their fixed connectivity and is reflected in the specific heat.

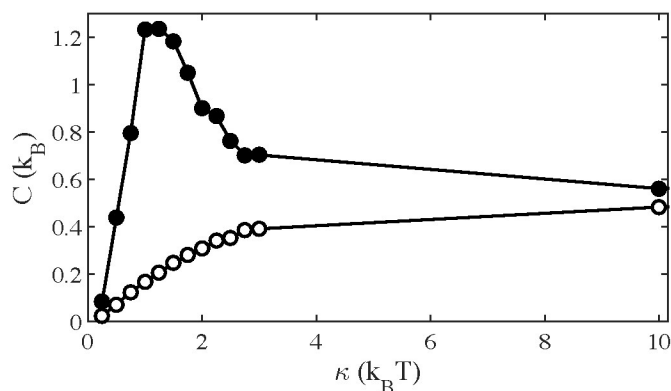


Fig. 2 Specific heat as a function of κ for fluid (filled circles) and non-fluid (open circles) membranes ($N = 1197$). The fluid membrane exhibits a peak in the specific heat near $\kappa = 1.25 k_B T$ that is characteristic of a transition from a branched-like state to an extended tube-like state.

3.3 Confined polymers suppress membrane fluctuations and can significantly deform the confining tube

Having characterized the equilibrium behavior of empty membrane tubes, we now investigate the effects of confining a semiflexible polymer inside. We focus primarily on the fluid membrane tube, since it exhibits nontrivial behavior as a function of bending rigidity and is biologically relevant. We begin by considering a membrane tube ($N = 1197$) with $\kappa = 1.25 k_B T$, which is near the peak in the specific heat (C), and investigate the effect of polymer length and persistence length on C . Polymers are constrained to span the tube, as discussed previously. Figure 4 demonstrates that confining a polymer within the membrane tube decreases the specific heat of the membrane compared with the

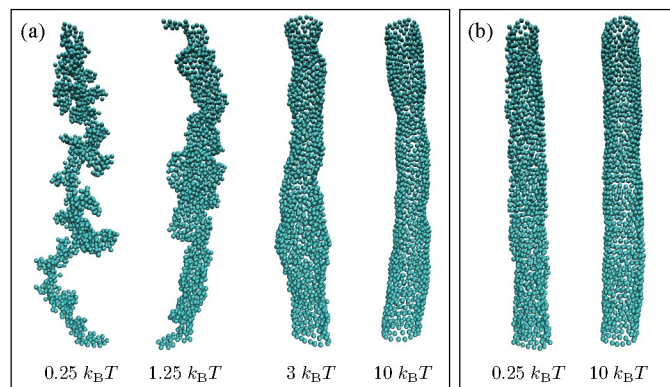


Fig. 3 (a) Equilibrium configurations of empty fluid membrane tubes ($N = 1197$) for $\kappa = 0.25, 1.25, 3, 10 k_B T$. At small values of κ , the membrane is characterized by large shape fluctuations. (b) Equilibrium configurations of empty non-fluid membrane tubes ($N = 1197$) for $\kappa = 0.25$ and $10 k_B T$. For clarity, only particles (and not bonds) are shown in the images.

empty tube. That is, the presence of a polymer suppresses the energy fluctuations of the membrane ($C \propto \langle (E_m - \langle E_m \rangle)^2 \rangle$). The decrease occurs for all polymers considered, with more pronounced effects for longer polymers and larger persistence lengths. Table 1 provides results over a wider range of polymer conditions and for an additional membrane tube size. Results are consistent with those shown in Fig. 4.

Figure 5 shows representative configurations of the polymer-membrane system for polymers of various lengths and persistence lengths confined within a fluid membrane tube with $\kappa = 1.25 k_B T$. When the polymer length is similar to the distance between the two sides of the tube, increasing persistence length leads to a curved, serpentine configuration. The polymer is not long enough to significantly deform the membrane by forming loops or localized structures, as these would incur large energy penalties from bending the polymer, so the polymer adopts curved shapes like those shown in the figure. As the polymer becomes longer, for sufficiently large persistence lengths, the polymer forms loops that

Table 1 Ratio of the specific heat of a membrane tube with a confined polymer to the specific heat of the corresponding empty membrane tube. The polymer size (M) and persistence length (l_p) are varied for two different membrane sizes.

N	M	l_p (μm)						
		0	15	30	60	90	120	240
798	50	0.84	0.81	0.82	0.78	0.78	0.79	0.78
	75	0.78	0.78	0.75	0.74	0.70	0.69	0.67
	100	0.75	0.73	0.72	0.68	0.65	0.68	0.63
	125	0.74	0.73	0.69	0.69	0.68	0.60	0.56
	150	0.57	0.47	0.43	0.40	0.38	0.37	0.31
1197	75	0.84	0.83	0.84	0.82	0.80	0.80	0.80
	125	0.78	0.79	0.76	0.75	0.73	0.68	0.68
	175	0.77	0.76	0.71	0.68	0.67	0.65	0.61
	225	0.75	0.72	0.66	0.66	0.65	0.62	0.58

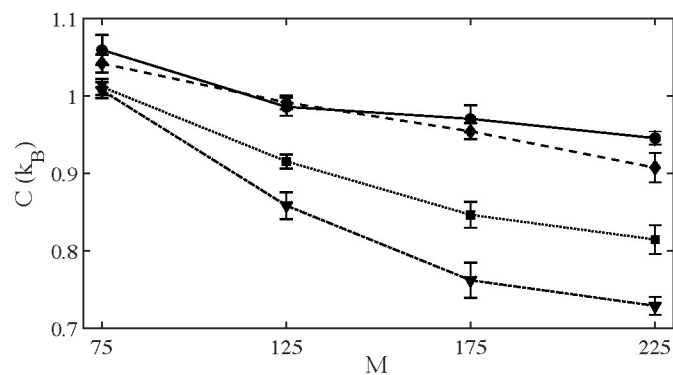


Fig. 4 Specific heat of the membrane ($N = 1197$) as a function of polymer length for various polymer persistence lengths. The bending rigidity is $\kappa = 1.25 k_B T$ and persistence lengths are $l_p = 0, 15, 90$ and $240 \mu\text{m}$ (circle, diamond, square, and triangle, respectively). Each point represents the average over 10 simulation trajectories, with error bars representing the standard error. The specific heat of the empty membrane tube is $1.24 k_B$.

cause localized, bulge-like deformations of the tube. At small values of persistence length, the energetic cost of forming a bulge in the membrane tube prevents large polymer loops from forming. Instead, smaller loops and locally deformed polymer shapes are seen, since these incur relatively small energetic costs and minimally deform the tubular membrane shape. Figure 5 also shows representative configurations of a non-fluid membrane tube with a polymer inside. The fixed connectivity of the non-fluid membrane prevents it from being significantly deformed by the polymer, and as such, stiff polymers adopt configurations with compact loops that are less energetically favorable than those in the fluid membrane case.

Figure 6 further investigates the effect of a confined polymer on the specific heat of a fluid membrane tube as a function of bending rigidity. The presence of the polymer decreases the specific heat of the membrane across the regime of κ in which the empty membrane tube exhibits a local maximum. Taken together, the results of this section indicate that confining a polymer within a fluid membrane tube suppresses shape fluctuations in the regime in which the empty membrane exhibits large fluctuations. This in turn is reflected in the specific heat, which decreases as a consequence of reduced energy fluctuations. At small values of the persistence length (e.g., $l_p = 0$), the polymer interacts with mem-

brane particles through hard-sphere interactions, partially filling the tube and inhibiting the creation of fingerlike projections, even though the polymer does not significantly deform the tube. At large values of the persistence length (for sufficiently long polymers), it is energetically favorable for a polymer to minimize its bending energy by forming a number of circular loops that are accommodated by a localized bulge in the membrane. The polymer prevents large fluctuations of the membrane in the bulged region, and the remaining membrane has relatively few total particles (i.e., surface area) with which it can sample configurations. This results in fewer accessible membrane shapes and hence a decrease in energy fluctuations. Note that it is possible for a polymer to form loops in two or more locations concurrently, with the loops causing a local deformation of the membrane at each location. For example, this is evident in Fig. 5 for the fluid membrane with $M = 175$ and $l_p = 15 \mu\text{m}$. For a long polymer with a large persistence length, a configuration with polymer loops in multiple locations would likely be metastable, with a single localized membrane deformation corresponding to the lowest energy state. However, excluded volume interactions between polymer particles, if taken into account, would likely prevent several loops from coexisting in a single region due to volume constraints, hence promoting the formation of loops in multiple locations. Configurations with multiple localized bulges would also suppress shape and energy fluctuations as a consequence of the polymer-induced membrane deformations, as discussed above.

Confining a polymer within a non-fluid membrane tube also decreases the specific heat of the membrane, but to a much lesser extent than for the fluid membrane tube. The Fig. 6 inset shows that for a fixed polymer length, increasing the persistence length of a polymer within a non-fluid membrane tube leads to relatively minor changes in the specific heat of the membrane. This is consistent with the simulation snapshots of non-fluid membrane tubes in Fig. 5, in which the polymer has a significantly less pronounced effect on the shape of the membrane than in the fluid membrane case.

To explore the transition in fluid membranes from an approximately cylindrical tube to a tube with a polymer-induced bulge, we calculate the energies of idealized membrane-polymer configurations. We consider two configurations representative of low-energy states that capture the basic physics of the polymer-membrane configurations: (i) a cylindrical tube with a helical polymer inside and (ii) a tube with a spherical bulge in which the polymer forms loops. The energy of the confined polymer is calculated using Eqn. 1 and the energy of the membrane is calculated using Eqn. 2. These results are expected to be most relevant when fluctuations do not play a significant role (i.e., when entropic contributions are a relatively unimportant part of the free energy). In the first case, we assume the tube is cylindrical with length L_T and radius R_c , and that the polymer (of length l) adopts a helical configuration within the tube. Although our simulations do not explicitly account for surface tension, the tube size is constrained by the number of particles and the maximum bond length. Hence, we constrain R_c to the maximum radius possible for a cylinder defined by initial conditions n_p and n_1 , $R_c = n_p l_{\text{max}} / 2\pi$, as this will minimize the energy of both the membrane and the polymer. The

polymer is described by

$$\mathbf{r}(s) = \begin{pmatrix} R_c \cos(\alpha s) \\ R_c \sin(\alpha s) \\ sL_T/l \end{pmatrix}$$

where $\alpha = \sqrt{(1 - (L_T/l)^2)/R_c}$ and $0 \leq s \leq l$. Using this expression for the polymer shape, the total energy can be written

$$E_1 = \frac{\pi\kappa L_T}{R_c} + \frac{l_p k_B T}{2} \frac{l}{R_c^2} \left(1 - \left(\frac{L_T}{l}\right)^2\right)^2$$

The first term accounts for the energy of the membrane and the second term accounts for the energy of the polymer. This function grows linearly with l_p with other parameters held fixed.

In the second membrane-polymer configuration, we assume that a spherical bulge of radius R_s is present in an otherwise cylindrical membrane. The polymer is assumed to be straight within the cylindrical region and to form circular loops of radius R_s in the spherical region. The length of the cylindrical portion is approximated as $L_T - 2R_s$, the bulged region is assumed to be a complete sphere, and the maximum possible surface area is given in relation to a corresponding discrete representation by $A_{\text{tot}} = 2n_p(n_p - 1)(l_{\text{max}}^2\sqrt{3}/4)$. Under the approximations described, the energy of the system is

$$E_2 = 8\pi\kappa + 2\pi^2\kappa \frac{(L_T - 2R_s)^2}{A_{\text{tot}} - 4\pi R_s^2} + \frac{l_p k_B T}{2} \left(\frac{l - (L_T - 2R_s)}{R_s}\right)$$

The first terms are associated with the spherical and cylindrical portions of the membrane, respectively, and the third term gives the energy of the polymer. For this system, we minimize the energy with respect to the bulge size (R_s) subject to the total area being as large as possible (a fixed surface area allows the radius of the cylinder to be written in terms of R_s above). Physically, increasing R_s decreases the polymer energy since larger loops can be formed, yet it leads to a smaller radius for the cylindrical portion of the membrane, thus increasing the membrane energy.

Figure 7 shows E_1 and E_2 as a function of the polymer persistence length for a membrane tube of fixed length. The polymer is twice the length of the tube in this example. For each value of κ considered, there is a crossover at which the spherical bulge case becomes energetically favorable compared with the cylindrical case. As expected, this transition occurs at larger values of the persistence length as κ increases since it becomes more energetically costly to deform the membrane. Although we are considering simple representative configurations, they capture the crossover to a deformed tube and likely incorporate the physical interactions most relevant at large κ .

Using computer simulations, we have also considered the effects of confined polymers when the polymer is not constrained to span the entire tube, with a focus on two cases: (i) both polymer ends are free to move anywhere within the tube, and (ii) one end of the polymer is constrained at a tube end and the other end is free. Both cases exhibit qualitatively similar behavior in which the specific heat of a fluid membrane is decreased by the polymer. However, the effects are most pronounced for the polymer that is

constrained to fully span the tube. This is because the partially constrained or unconstrained polymers adopt configurations that typically do not span the entire tube, and hence they directly interact with less of the membrane.

4 Discussion

Tubular membrane structures are common in cells and highlight important biophysical interactions between deformable membranes and semiflexible biopolymers such as actin. Models that capture elastic properties of both the polymer and the membrane allow us to investigate many important features of their interactions, namely that they are deformable, are subject to thermal fluctuations, and can mutually influence each other's behavior. The persistence length of a single actin filament is approximately 15 μm , although bundles of actin filaments, which are common in cells, have persistence lengths that grow with the number of actin filaments in the bundle.¹ Typical measurements of cell membranes give $\kappa \sim 10 - 20 k_B T$. However, many model bilayer systems exhibit bending rigidities above and below this range, and many can be tuned by controlling the relative quantities of bilayer components.^{26,34} The simulations in this paper are meant to characterize general features of polymer-membrane tube interactions in parameter regimes that are biophysically relevant.

We used Monte Carlo computer simulations to study the equilibrium behavior of tubular membrane structures with and without a semiflexible polymer confined inside of the tube. For empty fluid membrane tubes, we observed a local peak in the specific heat as the bending rigidity increases from zero. In the fluid membrane tubes, the peak in specific heat is associated with a transition from membrane structures with highly irregular shapes at small κ to extended, tube-like configurations at large κ . Non-fluid membranes, which have fixed connectivity of constituent particles, maintain extended tube-like behavior at all values of the bending rigidity.

We further observed that confining a semiflexible polymer within a fluid membrane tube results in a reduction of energy fluctuations of the membrane in the regime around the transition from irregular to tube-like membrane shapes. For polymers with a small persistence length, this is a consequence of excluded volume interactions that result in the polymer partially filling the tube and restricting the configurations available to the membrane. For stiff polymers, the energy associated with bending the polymer leads to an interesting interplay between the polymer and membrane. For polymers only slightly longer than the separation between the tube ends, we observed serpentine polymer-membrane shapes. This allows the polymer to span the tube without incurring large bending penalties associated with small loops or deformations. For longer polymers, localized bulges in the membrane accommodate polymer loops.

The results presented in this paper highlight nontrivial equilibrium behavior of tubular membranes in a regime of low bending rigidity. Additionally, we characterized two potentially biologically important roles of semiflexible polymers confined by membranes: (i) that they can suppress membrane shape fluctuations and (ii) that they can induce significant local deformations of the membrane. Due to the prevalence of membrane-confined

polymers within cells, we anticipate that these consequences of polymer-membrane interactions may play a role in a wide array of cellular structures.

5 Acknowledgments

We thank the University of Tennessee for financial support.

References

- 1 S. Pronk, P. L. Geissler and D. A. Fletcher, *Phys. Rev. Lett.*, 2008, **100**, 258102.
- 2 P. Cifra, Z. Benková and T. Bleha, *J. Phys. Chem. B*, 2008, **112**, 1367–1375.
- 3 Y. Yang, T. W. Burkhardt and G. Gompper, *Phys. Rev. E*, 2007, **76**, 011804.
- 4 P. Vázquez-Montejo, Z. McDargh, M. Deserno and J. Guven, *Phys. Rev. E*, 2015, **91**, 063203.
- 5 W. Reisner, J. N. Pedersen and R. H. Austin, *Rep. Prog. Phys.*, 2012, **75**, 106601.
- 6 F. Brochard-Wyart, T. Tanaka, N. Borghi and P.-G. de Gennes, *Langmuir*, 2005, **21**, 4144–4148.
- 7 A. J. Spakowitz and Z.-G. Wang, *Phys. Rev. Lett.*, 2003, **91**, 166102.
- 8 B. Onfelt, S. Nedvetzki, K. Yanagi and D. M. Davis, *J. Immunol.*, 2004, **173**, 1511–1513.
- 9 A. Rustom, R. Saffrich, I. Markovic, P. Walther and H.-H. Gerdes, *Science*, 2004, **303**, 1007–1010.
- 10 S. Sowinski, C. Jolly, O. Berninghausen, M. A. Purbhoo, A. Chauveau, K. Kohler, S. Oddos, P. Eissmann, F. M. Brodsky, C. Hopkins, B. Onfelt, Q. Sattentau and D. M. Davis, *Nat. Cell Biol.*, 2008, **10**, 211–219.
- 11 D. M. Davis and S. Sowinski, *Nat. Rev. Mol. Cell Biol.*, 2008, **9**, 431–436.
- 12 I. Derényi, F. Jülicher and J. Prost, *Phys. Rev. Lett.*, 2002, **88**, 238101.
- 13 G. Koster, A. Cacciuto, I. Derényi, D. Frenkel and M. Dogterom, *Phys. Rev. Lett.*, 2005, **94**, 068101.
- 14 Y. Li, R. Lipowsky and R. Dimova, *Proc. Natl. Acad. Sci. U. S. A.*, 2011, **108**, 4731–4736.
- 15 A. Roux, *Soft Matter*, 2013, **9**, 6726–6736.
- 16 D. R. Nelson, T. Piran and S. Weinberg, *Statistical Mechanics of Membranes and Surfaces*, World Scientific, Singapore, 2nd edn, 2004.
- 17 Y. Kantor and D. R. Nelson, *Phys. Rev. Lett.*, 1987, **58**, 2774–2777.
- 18 J.-S. Ho and A. Baumgärtner, *Europhys. Lett.*, 1990, **12**, 295–300.
- 19 A. Baumgärtner and J.-S. Ho, *Phys. Rev. A*, 1990, **41**, 5747–5750.
- 20 G. Gompper and D. M. Kroll, *J. Phys.: Condens. Matter*, 1997, **9**, 8795–8834.
- 21 H. Noguchi, *J. Phys. Soc. Jpn.*, 2009, **78**, 041007.
- 22 G. Gompper and D.M. Kroll, *J. Phys. I France*, 1996, **6**, 1305–1320.
- 23 L. Bagatolli and P. B. Sunil Kumar, *Soft Matter*, 2009, **5**, 3234–3248.
- 24 H. Noguchi and G. Gompper, *Proc. Natl. Acad. Sci. U. S. A.*, 2005, **102**, 14159–14164.
- 25 D. Kroll and G. Gompper, *Science*, 1992, **255**, 968–971.
- 26 D. H. Boal, *Mechanics of the Cell*, Cambridge University Press, Cambridge, 2nd edn, 2012.
- 27 P. A. Wiggins and P. C. Nelson, *Phys. Rev. E*, 2006, **73**, 031906.
- 28 Z. Yang, D. Zhang, L. Zhang, C. Hongping, A. ur Rehman and H. Liang, *Soft Matter*, 2011, **7**, 6836–6843.
- 29 T. Odijk, *Macromolecules*, 1983, **16**, 1340–1344.
- 30 E. Werner and B. Mehlig, *Phys. Rev. E*, 2014, **90**, 062602.
- 31 K. Avramova and A. Milchev, *J. Chem. Phys.*, 2006, **124**, 024909.
- 32 M. Fošnarič, A. Iglič, D. M. Kroll and S. May, *Soft Matter*, 2013, **9**, 3976–3984.
- 33 A. Šarić and A. Cacciuto, *Phys. Rev. Lett.*, 2012, **109**, 188101.
- 34 W. Rawicz, K. C. Olbrich, T. McIntosh, D. Needham and E. Evans, *Biophys. J.*, 2000, **79**, 328–339.

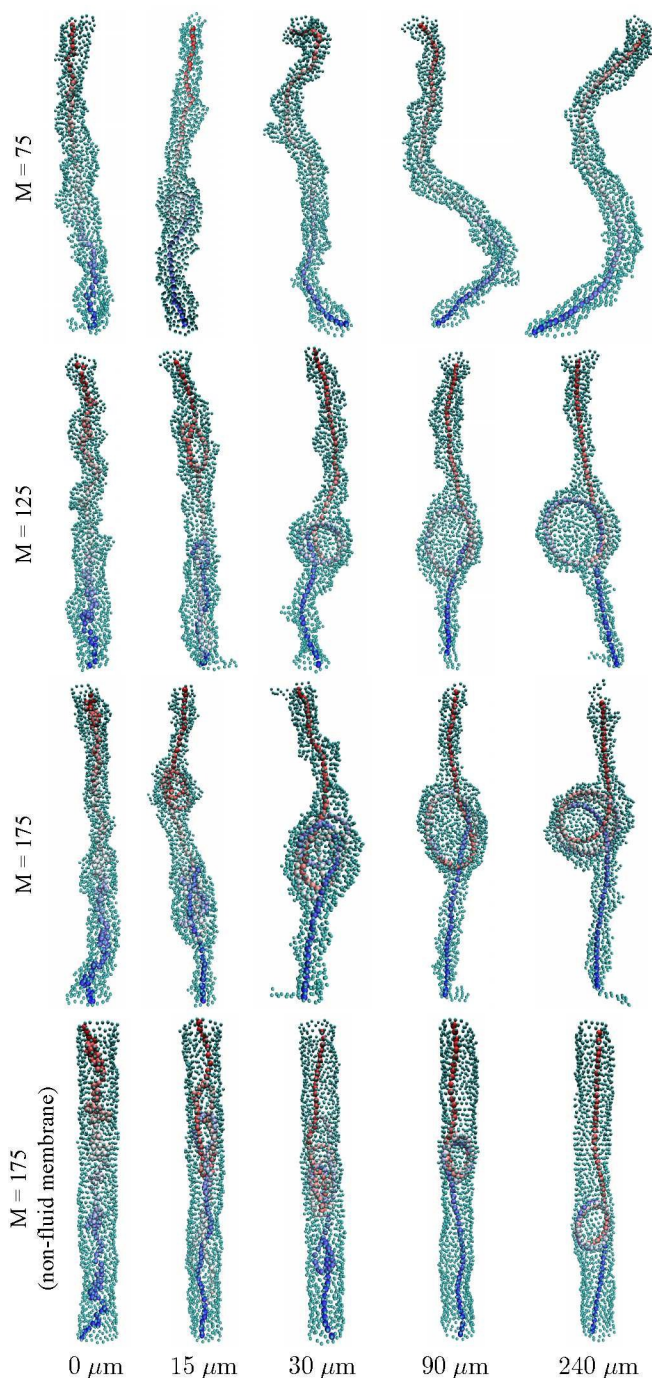


Fig. 5 Simulation snapshots of polymers confined within fluid and non-fluid membrane tubes. The bending rigidity of the membrane ($N = 1197$) is $\kappa = 1.25 k_B T$. Three polymer lengths (M) are shown at various values of the persistence length ($l_p = 0, 15, 30, 90, 240 \mu\text{m}$). The top three rows display fluid membrane tubes and the last row displays non-fluid tubes. From top to bottom, the ratio of $(M - 1)\bar{l}$ to the initial tube length is 1.4, 2.3, and 3.2. From left to right, the ratio of l_p to the initial tube length is 0, 0.21, 0.42, 1.3, and 3.4.

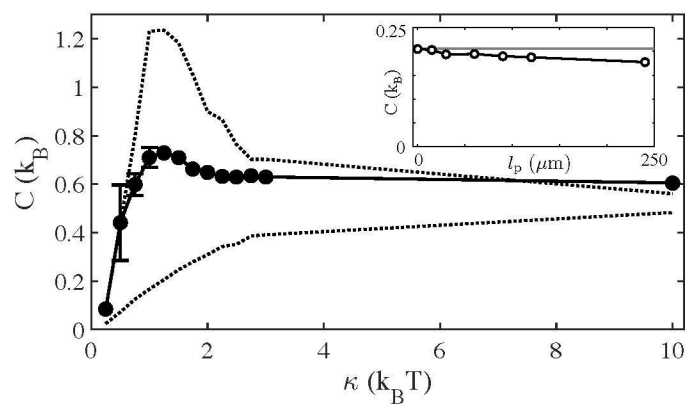


Fig. 6 Specific heat of the membrane as a function of bending rigidity for a fluid membrane tube with a polymer inside. The membrane ($N = 1197$) contains a polymer with $M = 225$ and $l_p = 240 \mu\text{m}$. Dashed lines highlight results for empty fluid (upper) and non-fluid (lower) membrane tubes (see Fig. 2). Averages are taken over 10 trajectories and error bars represent the standard error (points with no error bars have a standard error smaller than the size of the symbol). Inset: Specific heat of a non-fluid membrane tube ($N = 1197$) with $\kappa = 1.25 k_B T$ containing a polymer of length $M = 225$ (specific heat of the empty tube is shown as a horizontal grey line).

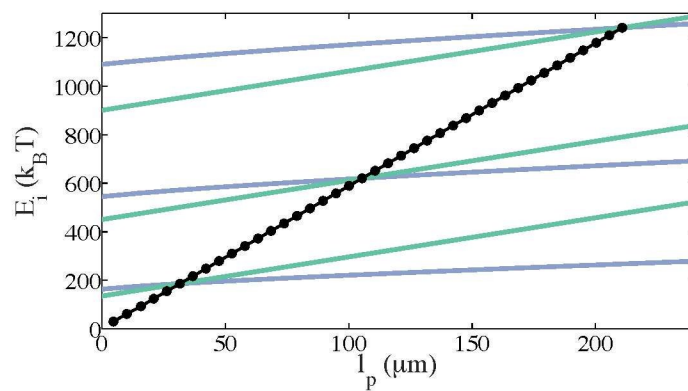
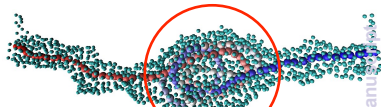
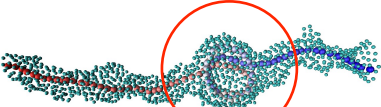
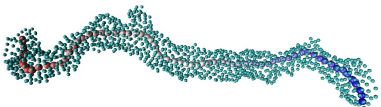
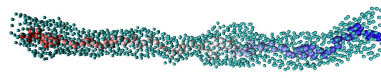
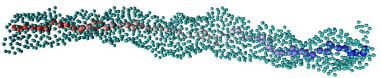


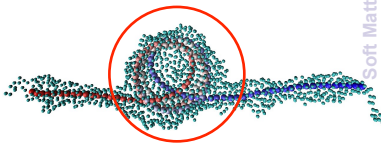
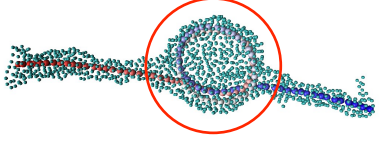
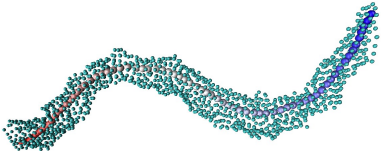
Fig. 7 Energy of idealized membrane-polymer configurations as a function of polymer persistence length. Results are shown for a cylindrical membrane with a helical polymer (green lines, $i = 1$) and a tube with a spherical bulge (blue lines, $i = 2$), for $\kappa = 3, 10, \text{ and } 20 k_B T$ (from bottom to top). The size of the spherical bulge (R_s) minimizes the energy E_2 . Black circles denote crossover points at which the configuration with a spherical bulge becomes energetically favorable (points correspond to $\kappa = 0.5, 1, 1.5, \dots, 20 k_B T$). Conditions in the figure correspond to a tube length of $L_T = 62(\sqrt{3}/2)\bar{l}$ with the polymer length $l = 2L_T$.

increasing persistence length



serpentine configuration

localized tube deformation



increasing polymer length